Science of the Total Environment 755 (2021) 143255

Contents lists available at ScienceDirect

Science of the Total Environment

journal homepage: www.elsevier.com/locate/scitotenv

# Hepatocellular carcinoma (HepG2/C3A) cell-based 3D model for genotoxicity testing of chemicals

Martina Štampar [a,b], Helle Sedighi Frandsen [c], Adelina Rogowska-Wrzesinska [c], Krzysztof Wrzesinski [d], Metka Filipič [a], Bojana Žegura [a,*]

[a] Department of Genetic Toxicology and Cancer Biology, National Institute of Biology, Ljubljana, Slovenia
[b] Jozef Stefan International Postgraduate School, Ljubljana, Slovenia
[c] Department of Biochemistry and Molecular Biology, University of Southern Denmark, Odense, Denmark
[d] CelVivo ApS 3D Structures, Blommenslyst, Denmark

## HIGHLIGHTS

- Hepatic 3D cell models have more complex structure and improved metabolic capacity compared to 2D.
- HepG2/C3A 3D model provide physiologically more relevant information for human exposure.
- Hepatic 3D cell model can contribute to trustworthy risk assessment genotoxic compounds.
- Dynamic HepG2/C3A 3D model enables prolonged exposures to low doses of xenobiotics.
- Comet assay was successfully implemented to the dynamic HepG2/C3A 3D cell model.

## GRAPHICAL ABSTRACT

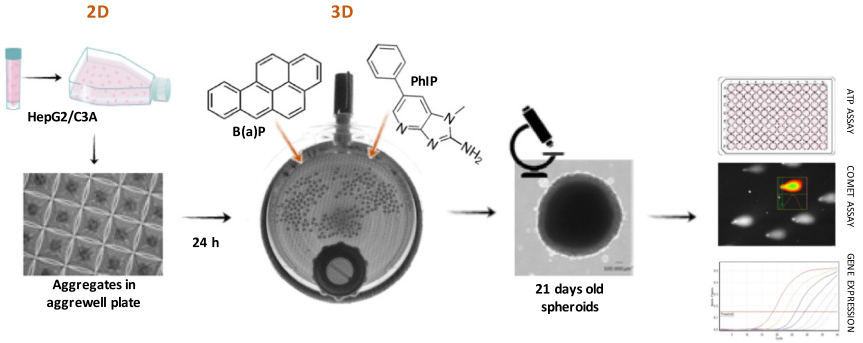


## ARTICLE INFO

*Article history:*
Received 21 September 2020
Received in revised form 22 October 2020
Accepted 24 October 2020
Available online 3 November 2020

Editor: Henner Hollert

*Keywords:*
*In vitro* 3D cell model
21-day old spheroids
Cytotoxic
Genotoxic
Gene expression

## ABSTRACT

The major weakness of the current *in vitro* genotoxicity test systems is the inability of the indicator cells to express metabolic enzymes needed for the activation and detoxification of genotoxic compounds, which consequently can lead to misleading results. Thus, there is a significant emphasis on developing hepatic cell models, including advanced *in vitro* three-dimensional (3D) cell-based systems, which better imitate *in vivo* cell behaviour and offer more accurate and predictive data for human exposures. In this study, we developed an approach for genotoxicity testing with 21-day old spheroids formed from human hepatocellular carcinoma cells (HepG2/C3A) using the dynamic clinostat bioreactor system (CelVivo BAM/bioreactor) under controlled conditions. The spheroids were exposed to indirect-acting genotoxic compounds, polycyclic aromatic hydrocarbon [PAH; benzo(a) pyrene B(*a*)P], and heterocyclic aromatic amine [PhIP]) at non-cytotoxic concentrations for 24 and 96 h. The results showed that both environmental pollutants B(*a*)P and PhIP significantly increased the level of DNA strand breaks assessed by the comet assay. Further, the mRNA level of selected genes encoding metabolic enzymes from phase I and II, and DNA damage responsive genes was determined (qPCR). The 21-day old spheroids showed higher basal expression of genes encoding metabolic enzymes compared to monolayer culture. In spheroids, B(*a*)P or PhIP induced compound-specific up-regulation of genes implicated in their metabolism, and deregulation of genes implicated in DNA damage and immediate-early response. The study demonstrated that this model utilizing HepG2/C3A spheroids grown under dynamic clinostat conditions represents a very sensitive

* Corresponding author at: National Institute of Biology, Department of Genetic Toxicology and Cancer Biology, Večna pot 111, 1000 Ljubljana, Slovenia.
*E-mail addresses:* martina.stampar@nib.si (M. Štampar), hellef@bmb.sdu.dk (H. Sedighi Frandsen), adelinar@bmb.sdu.dk (A. Rogowska-Wrzesinska), kwr@celvivo.com (K. Wrzesinski), metka.filipic@nib.si (M. Filipič), bojana.zegura@nib.si (B. Žegura).

https://doi.org/10.1016/j.scitotenv.2020.143255

and promising *in vitro* model for genotoxicity and environmental studies and can thus significantly contribute to a more reliable assessment of genotoxic activities of pure chemicals, and complex environmental samples even at very low for environmental exposure relevant concentrations.



## 1. Introduction

Cell-based assays play an important role in the drug development process and safety assessment of chemicals and drugs as a fast, cost-effective and straightforward approach to reduce animal testing (Burden et al., 2015; Pfuhler et al., 2020; Schechtman, 2002). Genotoxicity testing is an essential element of the safety assessment of nearly all types of compounds on the market. It is also a very important issue when evaluating the possible adverse health effects of complex environmental samples to which humans can be exposed in their everyday life, to avoid unforeseen genotoxic effects on human health and the environment as well (Dix et al., 2007). The testing begins with a series of *in vitro* bacterial and mammalian cell-based assays, and in case of positive results, it is followed by *in vivo* testing in rodents. However, *in vitro* genotoxicity tests with mammalian cells are prone to misleading results. One of the crucial elements contributing to a relatively high percentage of *in vitro* misleading results is an insufficient representation of enzymes implicated in the metabolism of genotoxic compounds in cell lines used for routine genotoxicity testing (Kirkland et al., 2007). Over the last two decades, test systems with human hepatocellular carcinoma-derived cell lines such as HepG2 with the retained activity of specific metabolic enzymes *in vitro* have been introduced to the routine genotoxicity testing (Shah et al., 2018; Yang et al., 2018). Traditionally, *in vitro* test systems are based on monolayer [two-dimensional (2D)] cell cultures, which are associated with inherent limitations (Edmondson et al., 2014; Wrzesinski and Fey, 2015). The most important is the lack of multiple biological functions such as cell-to-cell and cell-to-matrix contacts. These result in reduced cell differentiation, modified cell signalling pathways, and the reduced expression and activities of several hepatic enzymes implicated in the metabolism of xenobiotic substances (phase I and II enzymes) (Aucamp et al., 2017; Edmondson et al., 2014; Hurrell et al., 2019).

Furthermore, 2D cell cultures do not adequately mimic the natural cell microenvironment represented by surrounding extracellular matrix and nearby cells. The 3R's strategy (reduce, replace, refine), focus on the reduction and optimization of the use of animals for *in vivo* testing (Corvi and Madia, 2017; Pfuhler et al., 2009). To follow this strategy it is essential to develop alternative *in vitro* cell-based systems, which more realistically resemble *in vivo* cell behaviour and microenvironment and thus ensure additional predictive data compared to 2D conditions.

The hepatic 3D cell models exhibit a greater level of liver-specific functions, including metabolic enzyme activities. Furthermore, the cell morphology and their biochemical properties are more similar to *in vivo* tissues (Aucamp et al., 2017; Loessner et al., 2010). Spheroids represent a very promising 3D cell model that can be cultured under static or dynamic conditions, using many techniques, ranging from hanging drop cultures, spinner flasks, non-adhesive surfaces, micromoulding, NASA rotary system (developed by National Aeronautics and Space Administration), bioreactors, and many more (Basu et al., 2020; Breslin and O'Driscoll, 2013; Lin et al., 2008), each offering numerous advantages and disadvantages.

In addition to mechanistic studies (Elje et al., 2019; Mandon et al., 2019; Štampar et al., 2019), 3D models have also proven to be a very useful tool in environmental toxicology, including effect-based monitoring of various environmental natural and man-made pollutants (Basu et al., 2018; Hercog et al., 2020). The 3D models allow long-term repeat dose studies (Wong et al., 2011) enabling the exposure to lower concentrations of pollutants that are relevant for the environment and thus, real human exposure.

In the present study, the spheroids were developed using the advanced dynamic clinostat micro-tissue culturing technique, which applies rotating bioreactors, which provide better resemblance to *in vivo* conditions than 2D cell cultures (Fey and Wrzesinski, 2012; Wojdyla et al., 2016; Wrzesinski and Fey, 2015). The rotation of bioreactors causes the flow of growth media around the spheroids, resulting in higher diffusion of oxygen and nutrients into the spheroids and preventing the generation of a necrotic core (Fey and Wrzesinski, 2012; Gong et al., 2015; Lin et al., 2008). During prolonged culturing of several weeks, the spheroids develop structures with characteristics resembling tissues and stable physiological functionality such as bile canaliculi-like structures and sinusoid-like channels (Wrzesinski and Fey, 2013). Due to the advanced morphology and biochemical properties, the spheroids grown under dynamic conditions provide more predictive data for human exposure in comparison to classically cultured (2D) immortal or primary human hepatocytes and therefore represent an alternative approach for animal studies (Wrzesinski and Fey, 2013, 2015). Moreover, a dynamic clinostat micro-tissue culturing technique enables the formation of up to three hundred spheroids in one bioreactor at the same time (Fey and Wrzesinski, 2012) and thereby offers a simple high-throughput system for culturing uniform spheroids, where several down-stream techniques can be applied and various endpoint measured on the same population of spheroids that is particularly suitable in the environmental contamination studies.

This study aimed to develop an approach for genotoxicity testing of chemicals using 21-day old spheroids formed from human hepatocellular carcinoma (HepG2/C3A) cells utilizing the dynamic bioreactor (CelVivo BAM/bioreactor) system (Fig. 1). The age of 21 days was selected, since after this time the spheroids reach maturity and provide metabolically competent cell model (Fey and Wrzesinski, 2012; Wrzesinski et al., 2013; Wrzesinski and Fey, 2013). For the spheroid formation, the hepatocellular HepG2/C3A cell line (HepG2 cell subclone) was chosen due to its strong contact-inhibited growth characteristics, high transferrin and albumin production, alpha-fetoprotein synthesis, and the ability to grow in media containing a physiological level of glucose (Iyer et al., 2010; Sun et al., 2014; Tamta et al., 2012; Wrzesinski et al., 2013). When cultured in the form of spheroids HepG2/C3A cells have several advantages over other cell lines, such as reduced proliferation, the reestablishment of crucial functions (cholesterol and urea synthesis, cellular organization and expression of cytochrome P450) and can be utilised for studying long-term repeated dose exposures (Nibourg et al., 2012; Ramaiahgari et al., 2014; Wrzesinski and Fey, 2013). In addition, the HepG2/C3A spheroids have epigenetic markers that are present in the liver but are lost when cultured under 2D conditions (Tvardovskiy et al., 2015). However, recovery of physiological functions when grown in 3D is not limited to HepG2/C3A but is also seen with other cell lines, such as HepaRG, HepG2 and many others (Mandon et al., 2019; Štampar et al., 2019; Wrzesinski and Fey, 2013, 2015; Young and Young, 2019). The response of 21-day old HepG2/C3A spheroids for detection of indirect-acting genotoxic chemicals were tested with two model genotoxic compounds; benzo(*a*)pyrene (B(*a*)P) and 2-Amino-1-methyl-6-phenylimidazo(4,5-*b*)pyridine (PhIP) that are ubiquitously found in the environment and thus represent a risk for human health. Environmental pollution is a wide-reaching problem associated with the health of the ecosystem and humans, as well as global climate change (Hartig et al., 2014). Human

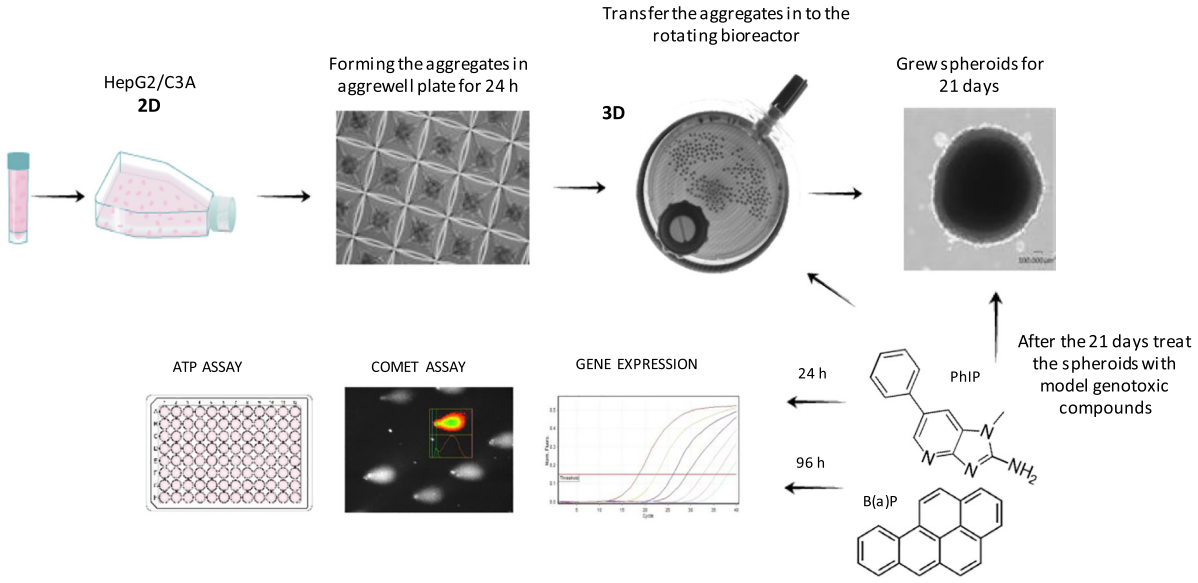


**Fig. 1.** The formation of the 3D HepG2/C3A spheroid cultures and treatment approach for genotoxicity assessment. First, the HepG2/C3A cells were seeded in the AggreWell™ plates and were left for 24 h at 37 °C. After that, the aggregates were transferred to the pre-wetted bioreactors. Spheroids were cultivated for 21 days until treated with B(*a*)p and PhIP for 24 and 96 h. After the treatment different end-point measurements were performed (cell viability, DNA damage and gene expression).

exposure to B(*a*)P is inevitable and is associated with pollution of the natural environment (water, air, soil), as well as with the intake of food, mainly grilled, charcoal-broiled, and smoked meat and fish (Baan et al., 2009). The second indirect-acting genotoxic chemical used in the present study belongs to the group of heterocyclic aromatic amines (HAAs) (Skog et al., 1998) and occurs in almost all types of food of animal origin (meat and fish) heated at high temperatures (Baird et al., 2005). PhIP has been detected not only in products of animal origin, but also in wine, beer (Manabe et al., 1993), and smoked cheese (Naccari et al., 2009), meaning that humans can be exposed to PhIP in their everyday environment due to their lifestyle. Moreover, it can occur in rainwater and cigarette smoke condensate (Naccari et al., 2009).

In the present study, the spheroids were exposed to BaP or PhIP for 24 and 96 h, and DNA damage was studied with the comet assay, which detects DNA lesions in the form of DNA strand breaks. To explore the metabolic competence of the spheroid model, the basal and induced mRNA level of genes, encoding selected enzymes implicated in xenobiotic metabolism induction, was determined. Besides, the effects of the tested compounds on deregulation of selected genes involved in the response to DNA damage and immediate-early response related to carcinogenesis were investigated.

## 2. Materials and methods

### 2.1. Chemicals

Dulbecco's Modified Eagle's Medium with 1 g Glucose/L (DMEM), GlutaMAX, Hanks' buffered saline solution and Trypsin-EDTA (10×; 0.50%) were from Gibco (Carlsbad, CA). Normal (NMP) and low (LMP) melting point agaroses, TRIzol® reagent and Trypan Blue (15250-061) were from Gibco (Praisley, Scotland, UK). Foetal calf serum (FCS), dimethylsulphoxide (DMSO), DEPC-treated water (w4502), non-essential amino acids (NEAA), penicillin/streptomycin (pen/strep), and benzo(*a*)pyrene (B(*a*)P; CAS-No. 50-32-8) were purchased from Sigma (St. Louis, USA). Cell-Titer-Glo luminescent cell viability assay (G7571) was obtained from Promega (Madison, USA). Amino-1-methyl-6-phenylimidazo[4,5-b] pyridine (PhIP; CAS-No. 105650-23-5) was from Toronto Research Chemicals Inc. (Canada). Methanol, ethanol, and phosphate-buffered saline (PBS) were from PAA Laboratories (Dartmouth, NH, USA). GelRed solution was from Biotium (Fremont, CA) and Triton X-100 from Fisher Sciences (New Jersey, USA). TaqMan Gene Expression Assays, the high capacity cDNA kit, and TaqMan Universal PCR Master Mix (4440038) were purchased from Applied Biosystems (New Jersey, USA). The PreAmp GrandMasterMix (TA05-50) was from TATAA Biocenter AB (Göteborg, Sweden). GE 48.48 Dynamic Array Sample and Assay loading Reagent Kit – 10 IFCs (85000821), and 48.48 Dynamic Array: Gene expression chip were obtained from Fluidigm (South San Francisco, USA). The B(*a*)P (9.9 mM) and PhIP (20 mM) stock solutions were prepared in DMSO and stored at −20 °C.

### 2.2. Cell culture

The immortalized human hepatocellular carcinoma cell line, HepG2/C3A, was bought at American Type Culture Collection (ATCC, CRL-10741). Cells were grown at standard culture conditions as described by Wrzesinski and Fey (2013) in DMEM (31885-023) supplemented with 10% FCS (Sigma F7524), 0.5% pen/strep (15140-122), 1% NEAA (11140-035), 1% GlutaMAX (35050-038), at 37 °C, 5% $CO_2$ atmosphere (Wrzesinski and Fey, 2013). HepG2/C3A cells were used between passage 6 and 9 and were regularly checked for mycoplasma (MycoAlert™ kit; Lonza, Walkersville, MD, USA).

### 2.3. Development of 3D spheroids and culture conditions

The spheroids made of HepG2/C3A cells were created using AggreWell™ 400 plates (Stemcell Technologies, 27845) as described by Wrzesinski and Fey (2013). In brief, the plates were first prewashed with the DMEM growth medium. Subsequently, the air bubbles were cleared away from the well surfaces by prefilling the plates with growth medium (0.5 ml) and centrifuging for 3 min at 3000*g*. Subsequently, $1.2 \times 10^6$ cells were added to the well resulting in 1000 cells per spheroid initially. The plates were centrifuged for 3 min at 100*g* and left overnight for spheroid formation. After the formation of spheroids, they were detached from the AggreWell™ plate by washing the well with growth medium pre-warmed to 37 °C and subsequently collected into a Petri-dish, and their quality was examined by microscopy (Olympus IX81, 4x). Cell aggregates, unlike the major population, if

any, have been removed to facilitate uniformity and the remaining spheroids were transferred, with cut p200 pipette tips, into the pre-equilibrated bioreactors (CelVivo BAM/bioreactor), which was subsequently filled with growth medium. The spheroids were cultured at 37 °C and 5% $CO_2$ for 21 days, replacing medium accordingly to 48/48/72 hour schedule (Fey and Wrzesinski, 2012). The day of the transfer of cell aggregates from AggreWell™ plates into the bioreactors is defined as day 0 (Wrzesinski and Fey, 2013). Optimal growth conditions were achieved by rotating bioreactors at appropriate speeds using the 16 axels BioArray Matrix drive BAM v4 (CelVivo, Blommenslyst) (Wojdyla et al., 2016).

### 2.4. Treatment of HepG2/C3A spheroids with model genotoxic compounds

After the spheroid cultures were matured for 21 days in bioreactors, spheroids have been divided into experimental subpopulation (50 spheroids in each bioreactor). The spheroids were treated with indirect-acting genotoxic compounds, namely polycyclic aromatic hydrocarbon benzo(*a*)pyrene (B(*a*)P) and heterocyclic aromatic amine amino-1-methyl-6-phenylimidazo[4,5-*b*]pyridine (PhIP) for 24 and 96 h. The spheroid size corresponded to approximately 9 million cells or 1.5 mg protein after 24 h of exposure and approximately 7 million cells or 1 mg protein after 96 h of exposure. The protein content was calculated from the standard curve (planimetry standardised table historical data) correlating the protein content and spheroid size. To initiate the chemical treatment, the rotation of bioreactors was terminated for a short time to allow the spheroids to descend to the bottom of the bioreactor. The media was replaced with fresh media containing B(*a*)P or PhIP. The concentrations of B(*a*)P and PhIP in the treatment media were adjusted to doses resulting in spheroids exposure to 0.15 and 0.011 μg B(*a*)P/μg cellular protein (corresponding to 40 and 4 μM) for 24 (short term) and 96 h (long term), respectively or 0.34 and 0.68 μg PhIP/μg cellular protein (corresponding to 200 and 400 μM) for 24-hour exposure and 0.246 μg PhIP/μg protein (corresponding to 100 μM) for 96-h. The dose is given as μg of chemical per μg of cellular protein (μg/μg P). The unit was converted from the concentration (mM) to the dose (*e.g.*, mg compound per mg cellular protein) based on the size of spheroids (Fey and Wrzesinski, 2012; Piccinini et al., 2015; Wrzesinski and Fey, 2015). The doses of genotoxins were selected according to previous studies with 2D models of HepG2 cells (Gajski et al., 2016; Pezdirc et al., 2013). The solvent (medium containing DMSO) and negative (growth medium) controls were included in all experiments. The final solvent dose was adjusted to be the same as the amount of the solvent in the exposure conditions. The experiments were performed in three independent repetitions and several spheroids were used for each time point and dose. The number of spheroids depended on the end-point evaluated.

### 2.5. Measurement of the surface area of spheroids (planimetry)

Spheroids were cultivated under dynamic clinostat conditions for 21 days, as described previously. Before and after the treatment, the quality, compactness, size, and roundness of at least 15 spheroids were documented at 4× magnification by light microscopy (Olympus IX81 motorized microscope). The images of spheroids were taken with the Olympus DP71 camera and analysed with Olympus AnalySiS Docu program (Soft Imaging System) where the spheroid area was measured in $\mu m^2$. This procedure was described in details by Fey and Wrzesinski in 2012.

### 2.6. Viability of spheroids after the treatment with genotoxic compounds – ATP assay

The 21-day old spheroids were treated with indirect-acting model genotoxins, B(*a*)P and PhIP, for 24 (short term) and 96 h (long term) in rotating bioreactors. In each bioreactor, 50 spheroids were grown. The viability of cells in spheroids was assessed after the treatment by measuring the ATP content of spheroids referring to the manufacturer's protocol (CellTiter-Glo, Cat. no. G7571) with minor modifications described by Wrzesinski and Fey (2013). Briefly, five spheroids from each treatment were collected at specific time points and each transferred to a well of microtiter plates (Nunc, 165306). The final volume of the growth medium was 100 μl, and spheroids were lysed by shaking in the darkness (40 min). Luminescence was determined using the FluoStar Omega® luminometer (BMG Labtech, Germany). Three independent experiments were performed. Data were normalized to the reference ATP standard curve, to the untreated control, and the surface area of each spheroid (determined with planimetry). Statistical relevance between solvent control and treated groups was calculated by unpaired parametric *t*-test with Welch's correction ($^*p < 0.05$).

### 2.7. DNA damage induced by genotoxic compounds – comet assay

After the treatment, a suspension of viable single cells was obtained by the combination of enzymatic digestion and mechanical degradation. Each spheroid was put in trypsin-EDTA (0.05%; 3 min) and afterwards, using cut pipette tips, disassembled into a suspension of single cells. The viability of the single cells was immediately evaluated by staining with Trypan Blue (0.4%). The comet assay was conducted according to Štraser et al. (2011) with modifications by Štampar et al. (2019). The images were captured with the fluorescence microscope Eclipse 800 (Nikon, Japan) with a Basler camera and analysed using Comet IV image analysis software (Perceptive Instruments, UK). Each spheroid represented one unit, and at least four spheroids were investigated per experimental point. In each spheroid, 50 randomly captured nuclei were analysed, and experiments were repeated three times independently. The results are shown as % of tail DNA. Statistic calculations were done by one-way ANOVA using Dunnett's Multiple Comparison test to test the differences in % of tail DNA of treatments *vs* control, and to compare the treated groups to solvent control ($^*p < 0.01$).

### 2.8. Gene expression analysis

The expression of studied genes involved in the metabolism of xenobiotics, immediate-early response and response to DNA damage were determined by quantitative real-time PCR (qPCR) on gene expression 48.48 Dynamic Array™ IFC (Fluidigm, US). The basal mRNA level of studied liver-specific and metabolic genes was determined in HepG2/C3A monolayers (2D) cultured for 48 h and in spheroids (3D) cultured for 22 and 25 days in bioreactors under dynamic conditions. Further, the expression of studied metabolic genes and genes encoding response to DNA damage and immediate-early response were evaluated in 21-day old spheroids exposed to B(*a*)P (0.15 μg/μg P and 0.011 μg/μg P for 24 and 96 h, respectively) or PhIP (0.34, 0.68 μg/μg P and 0.25 μg/μg P for 24 and 96 h, respectively). From the pool of 25 spheroids for each genotoxic compound and control, the mRNA was isolated using TRIzol Gibco BRL. The mRNA concentration and the purity were assessed using NanoDrop 1000 Spectrophotometer (Thermo Fischer Scientific, Wilmington, USA), while degradation was checked by gel-electrophoresis (BioRad Power PAC 3000 and UVP Chem Studio PLUS, Analytik Jena AG, US). Reverse transcription of total mRNA (1 μg) per sample was performed using the cDNA High Capacity Archive Kit. Quantification of studied genes was determined with qPCR on 48.48 Dynamic Array™ IFC method where TaqMan Universal PCR Master Mix and pre-amplificated (TATAA PreAmp GrandMasterMix) Taqman Gene Expression Assays listed in Table 1 were applied. All genes were preamplified. To eliminate the effects of inhibition and to evaluate the performance of the primer set, a serial of 5-fold dilutions of each target gene was analysed. The qPCR experiments were run on 48.48 Dynamic Array™ IFC chips for gene expression on the BioMark HD machine system (Fluidigm, UK). The program QuantGenious was used for data processing using the relative quantification regarding solvent control (Baebler

**Table 1**
The list of Taqman gene expression assays.

| | | Gene symbol | Entire gene name | Assay ID |
|---|---|---|---|---|
| Cellular function | Reference genes | *GAPDH* | Human Endogenous Control | Hs99999905_m1 |
| | | *HPRT1* | Hypoxanthine phosphoribosyl transferase 1 | Hs02800695_m1 |
| | DNA-damage response genes | *TP53* | Tumour protein P53 | Hs00153349_m1 |
| | | *MDM2* | Oncogene, E3 ubiquitin-protein ligase | Hs00234753_m1 |
| | | *GADD45α* | Growth arrest and DNA damage-inducible gene, alpha | Hs00169255_m1 |
| | | *CDKN1A* | Cyclin dependent kinase inhibitor 1A0 | Hs00355782_m1 |
| | | *ERCC4* | Excision repair cross-complementing rodent repair deficiency, complementation group 4 | Hs00193342_m1 |
| | Immediate-early response genes | *JUNB* | JunB proto-oncogene, AP-1 transcription factor subunit | Hs00357891_s1 |
| | | *MYC* | V-myc avian myelocytomatosis viral oncogene homolog | Hs00153408_m1 |
| | Genes involved in metabolism | *CYP1A1* | Cytochrome P450 family 1 subfamily A member 1 | Hs01054797_g1 |
| | | *CYP1A2* | Cytochrome P450 family 1 subfamily A member 2 | Hs00167927_m1 |
| | | *CYP3A4* | Cytochrome P450 family 3 subfamilies A member 4 | Hs02514989_s1 |
| | | *UGT1A1* | *UDP glucuronosyltransferase 1 family, polypeptide A1* | *Hs02511055_s1* |
| | | *UGT2B7* | UDP glucuronosyltransferase family 2 member B7 | Hs00426592_m1 |
| | | *NAT1* | *N*-acetyltransferase 1 | Hs02511243_s1 |
| | | *NAT2* | *N*-acetyltransferase 2 | Hs01854954_s1 |
| | | *SULT1B1* | Sulfotransferase family 1B member 1 | Hs00234899_m1 |
| | | *SULT1C2* | Sulfotransferase family 1C member | Hs00602560_m1 |
| | Hepatic markers | *ALDH3A1* | Aldehyde dehydrogenase 3 family member A1 | Hs00964880_m1 |
| | | *ALB* | Albumin | Hs00910225_m1 |

et al., 2017). If the difference was higher/lower than 1.5-fold, than the expression was considered as up/down-regulation (relative expression >1.5 or <0.66 fold change, respectively). The inverse value of the relative expression (1/RE) was calculated, to acquire a fold change from the relative expression for down-regulated genes (RE < 1). The expression of each gene was assessed in duplicates and three experiments were done independently. Statistical analysis was done by the multiple unpaired *t*-tests with the Sidak-Bonferroni method ($^*p < 0.05$).

## 3. Results and discussion

*In vitro* 3D cell cultures are experimental models increasingly used in preclinical studies, pharmacology, and toxicology. Recently, they have been applied also for studying the adverse effects of natural toxins and complex environmental samples and proved to be a very sensitive model (Basu et al., 2018; Flampouri et al., 2019; Hercog et al., 2020).

In genetic toxicology, the use of 3D culture models is still in its infancy, but at a recent International Workshop on Genotoxicity Testing (IWGT), their use for genotoxicity testing was recognized as very promising (Pfuhler et al., 2020). However, for the use in routine genotoxicity testing, further development and validation is needed (Pfuhler et al., 2020). In the present study, we established and validated a genotoxicity test system with 21-day old spheroids developed from the HepG2/C3A cell line that enables short-term and long-term exposure to xenobiotic pollutants under controlled dynamic clinostat conditions. One of the very important and crucial issues in genotoxicity studies is that the applied model enables long-term and repeated exposures to low doses of studied compounds, which is very important for the risk assessment of environmental contaminants. Namely in the environment, animals and humans can be continuously and/or repeatedly exposed to very low concentrations of various compounds.

### 3.1. The influence of model genotoxic compounds on HepG2/C3A spheroid growth and viability of cells

To determine the influence of B(*a*)P and PhIP on the growth of 21-day old spheroids, the surface area (planimetry) of at least 15 spheroids per experimental point was measured after 24 and 96 h of exposure (Fig. 2). The average surface area of spheroids exposed to B(*a*)P was affected after 24 h (0.15 μg/μg P) and 96 h (0.01 μg/μg P) exposure. After 24 hour and 96 hour exposure, the surface area was 0.97 ± 0.19 $mm^2$ and 0.98 ± 0.07 $mm^2$, respectively, while the surface area of the control group was 1.23 ± 0.11 $mm^2$ and 1.14 ± 0.23 $mm^2$, respectively. The results of PhIP exposure revealed that the heterocyclic aromatic amine (HAA) affected the growth of HepG2/C3A spheroids only after short (24 h) exposure. The surface area of spheroids exposed to PhIP at the dose of 0.34 and 0.68 μg/μg P was 1.20 ± 0.10 $mm^2$ and 1.17 ± 0.07 $mm^2$, respectively, while the average control surface area was 1.27 ± 0.11 $mm^2$ and 1.23 ± 0.11 $mm^2$, respectively, after a short exposure. After 96 hour exposure to 0.246 μg/μg P of PhIP, the surface area was 1.16 ± 0.13 $mm^2$ and in control group 1.14 ± 0.23 $mm^2$.

The effect of B(*a*)P and PhIP on the viability of HepG2/C3A spheroids was determined by measuring ATP content. The results showed that B(*a*)P and PhIP after 24 h at higher dose, reduced ATP content for 16.5% and 24.4% on average, respectively, while PhIP at lower dose did not affect the cell viability (Fig. 3A). After 96 h of exposure B(*a*)P or PhIP did not decrease the ATP content (Fig. 3B). As the reduction of ATP content at applied doses was less than 30%, which is considered as non-cytotoxic effect (Žegura et al., 2009), no significant disturbances of mitochondrial functions were expected; therefore, these doses were used for further experiments.

Recently it was described that cell viability of HepG2 spheroids cultured for 3 days under static conditions, exposed to B(*a*)P (up to 40 μM) for 24 h was not affected in their cell viability measured by MTS assay, while PhIP (≥ 200 μM) decreased cell viability by approximately 20% on average (Štampar et al., 2019). Similarly, in 10-day old HepaRG spheroids after 24 h of exposure, B(*a*)P at concentrations of up to 20 μM did not decrease cell survival, while cytotoxic effects were described for PhIP (≥ 320 μM) (Mandon et al., 2019).

### 3.2. The influence of model genotoxic compounds on DNA damage induction determined with the comet assay

Comet assay was recently applied in various hepatic 3D cell models (Elje et al., 2019; Mandon et al., 2019; Štampar et al., 2019), and here we successfully implemented the method on 21-day old HepG2/C3A spheroids grown under dynamic clinostat conditions. The spheroids were treated with B(*a*)P and PhIP for 24 and 96 h, and first, the method for obtaining the viable single-cell suspension was optimized. Before conducting the comet assay, the viability of single-cell suspension was determined by Trypan blue staining, and it was higher than 80% (data not shown). Results showed that B(*a*)P (0.15 μg/μg P) and PhIP (0.34 μg/μg P and 0.68 μg/μg P) after 24 h of treatment induced statistically significant increase in the amount of DNA strand breaks (Fig. 4A

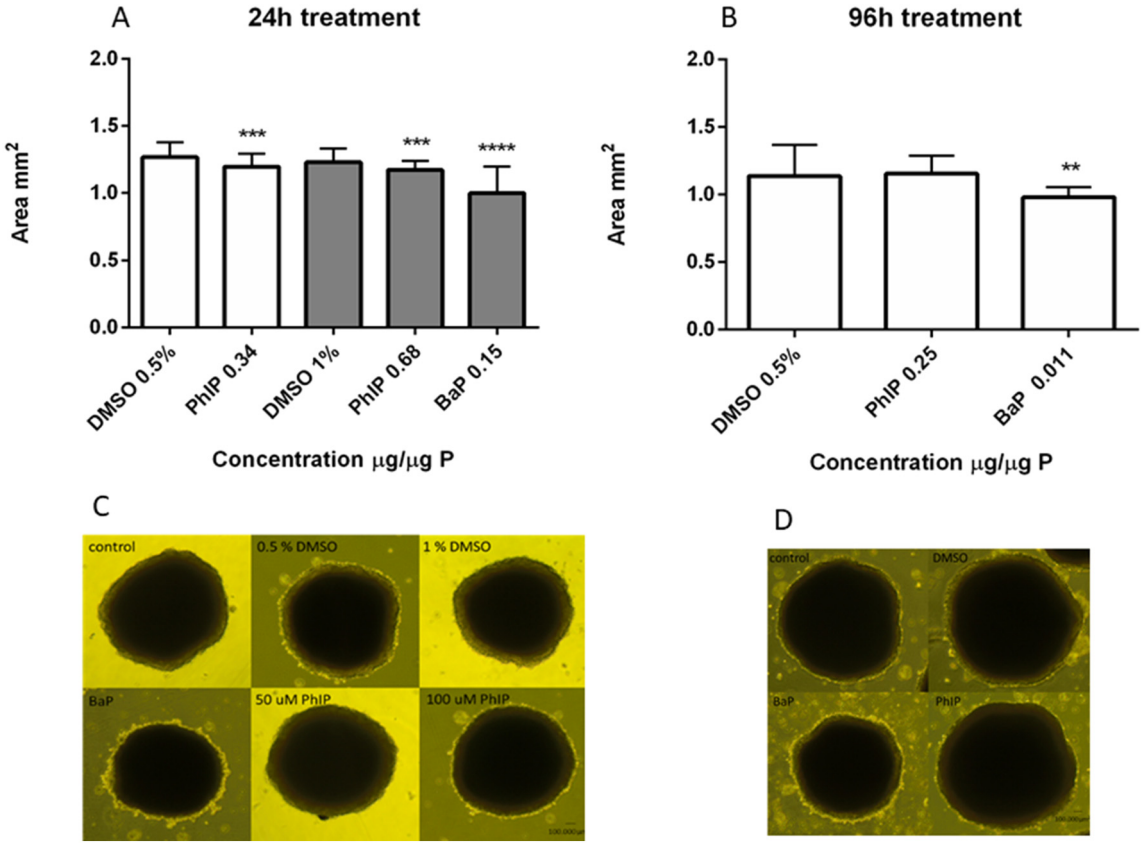


**Fig. 2.** The average surface area ± SD ($mm^2$) of control and exposed spheroids after 24 h (A) and 96 h (B) determined with planimetry. The % of the solvent in different treatments after 24 h was adjusted to the 0.5% at a lower dose of PhIP (white columns) and the 1% at the higher dose of PhIP and B(*a*)P (grey columns). The experiments were repeated three times independently and each time at least five spheroids were measured. The % of the solvent after 96 h was adjusted to 0.5%. The images of representative spheroids after 24 h (C) and 96 h exposure (D) are shown. The images were captured using the Olympus IX81 microscope and an Olympus DP71 camera at 4× magnification. Statistics analysis was conducted in Graph Pad Prism 6 (unpaired parametric *t*-test with Welch's correction).

and B). Similar results have been reported for HepG2 spheroids grown under static conditions that were exposed to B(*a*)P (≥ 10 μM) and PhIP (≥ 50 μM) for 24 h (Štampar et al., 2019). In line with our results, induction of DNA damage has also been observed in HepaRG spheroids exposed to B(*a*)P at ≥20 μM and PhIP at ≥40 μM as well as other pro-genotoxic compounds including cyclophosphamide, 7,12-dimethylbenz[*a*]anthracene, 2-acetylaminofluorene and acrylamide with the exception of 2-amino-3-methylimidazo[4,5-*f*]quinolone (Mandon et al., 2019). Comet assay on HepG2 spheroids has also been applied to assess genotoxicity of the direct-acting compounds methyl

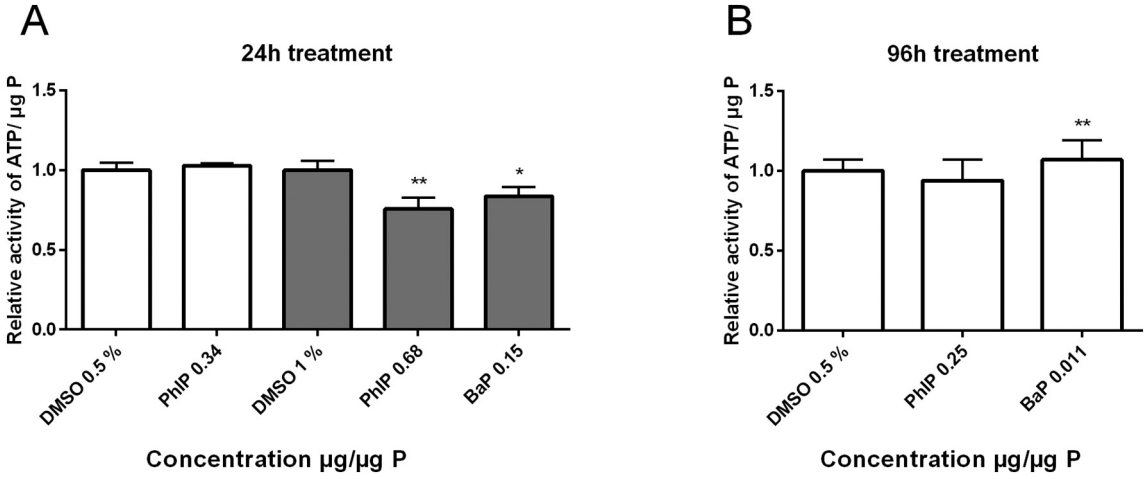


**Fig. 3.** The relative ATP content in HepG2/C3A spheroids (3D) after 24 (A) and 96 (B) hour treatment to B(*a*)P and PhIP determined with the ATP assay. Three independent experiments were performed and each time five spheroids from each bioreactor were collected at specific time points. The % of the solvent in different treatments after 24 h was adjusted to the 0.5% at a lower dose of PhIP (white columns) and to the 1% at the higher dose of PhIP and B(*a*)P (grey columns). The % of the solvent after 96 h was adjusted to 0.5%. Results are presented as relative ATP/μg protein ± SD normalized to corresponding solvent control. The statistical analysis was conducted in Graph Pad Prism 6 (unpaired parametric *t*-test with Welch's correction).

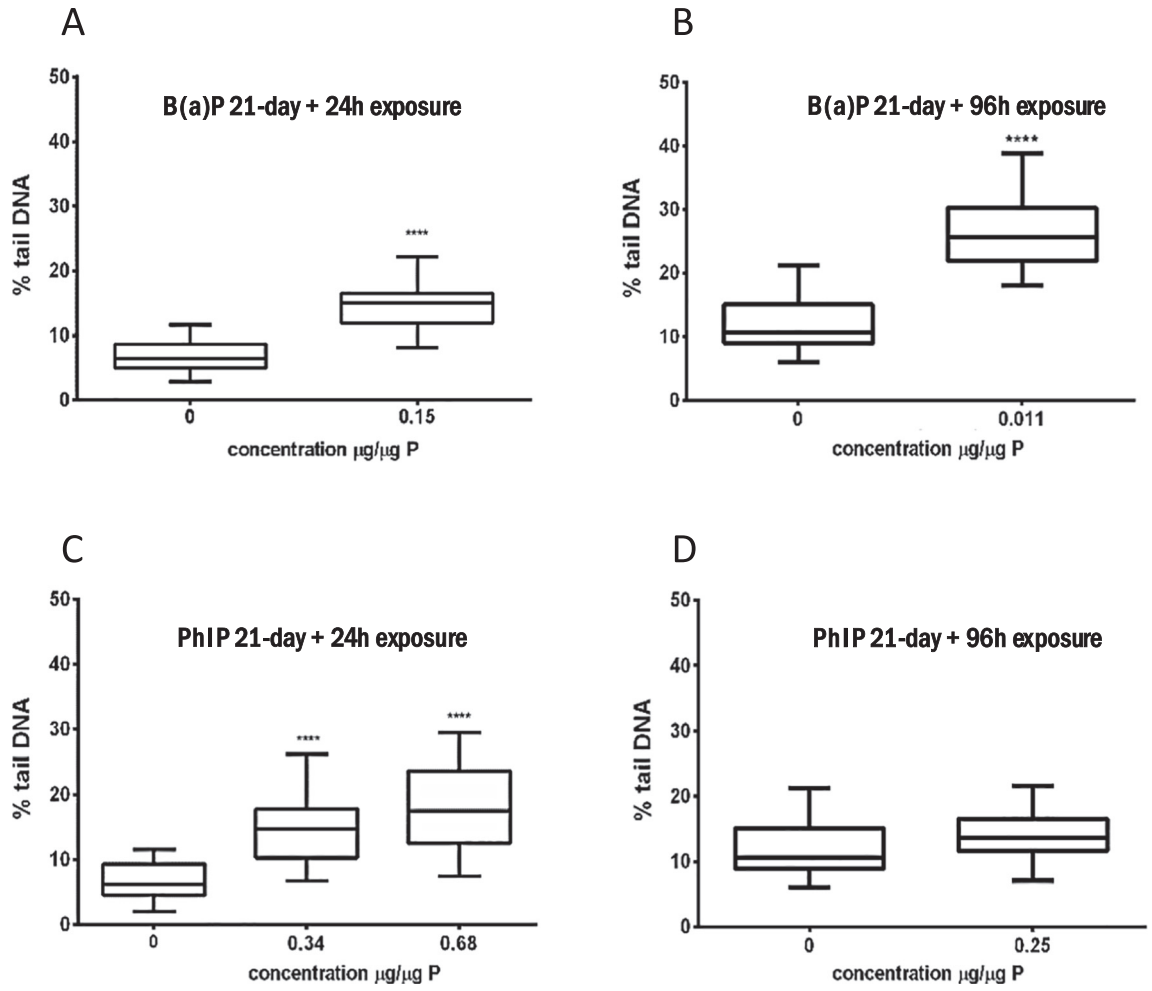


**Fig. 4.** Determination of DNA damage after the exposure of HepG2/C3A spheroids to indirect-acting model genotoxic compounds B(*a*)P and PhIP and solvent control (0) for 24 and 96 h by the comet assay (% tail DNA). Fifty nuclei were measured per experimental point and presented in box-plots. Three independent experiments were performed. (One-way ANOVA, Dunnett's test; **** $p < 0.001$).

methane sulfonate and hydrogen peroxide by Elje et al. (2019). After prolonged exposure (96 h) of HepG2/C3A spheroids to B(*a*)P, DNA damage was observed at approximately 10-times lower doses (0.011 µg/µg P) compared to doses used for 24 hour exposure (Fig. 4D), indicating high sensitivity of the system for detecting B(*a*)P genotoxicity. On the contrary, PhIP did not induce DNA damage in HepG2/C3A spheroids (Fig. 4C) after prolonged exposure to doses of 0.246 µg/µg P. The explanation for the observed effect can be the metabolism of PhIP after prolonged exposure and/or repair of DNA damage within 96 h of exposure as HepG2/C3A spheroids have been shown to have a very high level of DNA repair enzymes (Wrzesinski et al., 2014). It is also possible that the used dose of PhIP was too low to induce DNA damage although it was only 25% lower than the dose used for 24 hour exposure (0.246 µg/µg P *vs.* 0.34 µg/µg P, respectively).

### 3.3. Gene expression

#### 3.3.1. Basal mRNA expression in 3D compared to 2D monolayer system

The basal mRNA expression of studied liver-specific and phase I and phase II metabolic enzymes was determined in HepG2/C3A spheroids cultivated for 22 days (21 days plus additional 24 h) and 25 days (21 days plus additional 96 h). In HepG2/C3A monolayer cultures (2D), mRNA expression was determined after 2 days (1 day plus additional 24 h) of cell cultivation. The mRNA expressions of *albumin* (1.4-fold and 2.2-fold, respectively), *ALDH3A1* (3.5-fold and 1.6-fold, respectively) and metabolic enzymes of phase I, *CYP3A4* (1.1-fold and 3.2-fold, respectively), *CYP1A1* (3.5-fold and 2.5-fold, respectively), and phase II, *UGT2B7* (2.2-fold and 1.6-fold, respectively) *and SULT1C2* (3.4-fold and 5.9-fold, respectively), were up-regulated after 22 days and 25 days of cultivation compared to the 2D system cultured for 2 days (Fig. 5). The obtained results are in line with observations described by Štampar et al. (2019), and Shah et al. (2018) who demonstrated that HepG2 spheroids grown under static conditions expressed higher mRNA levels of metabolic enzymes, which is a crucial physiological function of hepatocytes *in vivo* (Snykers et al., 2009). Similarly, higher mRNA levels of genes encoding phase I and II drug-metabolizing enzymes (Ramaiahgari et al., 2014; Whitlock, 1999), nuclear receptors and xenobiotic transcription factors (Hurrell et al., 2019; Ramaiahgari et al., 2014, 2017) as well as a time-dependent increase of *albumin* (Ramaiahgari et al., 2014) was described in HepG2 spheroids, when compared to monolayer cultures. We have noticed that the basal mRNA levels of *UGT1A1* (0.5-fold and 0.6-fold, respectively) and *NAT2* (0.2-fold and 0.26-fold, respectively) were expressed to a lower extent in the dynamic clinostat 3D HepG2/C3A cell system compared to 2D cell culture (Fig. 5), while the expressions of *SULT1B1* (1.3-fold and 1.09-fold, respectively) and *NAT1* (0.85-fold and 1.15-fold, respectively) were not biologically importantly deregulated. Previously, Chang and Hughes-Fulford (2009) showed that the expression of metabolic and synthetic functional genes changes differently with the time of cultivation in 3 to 7-day old HepG2 spheroids when compared

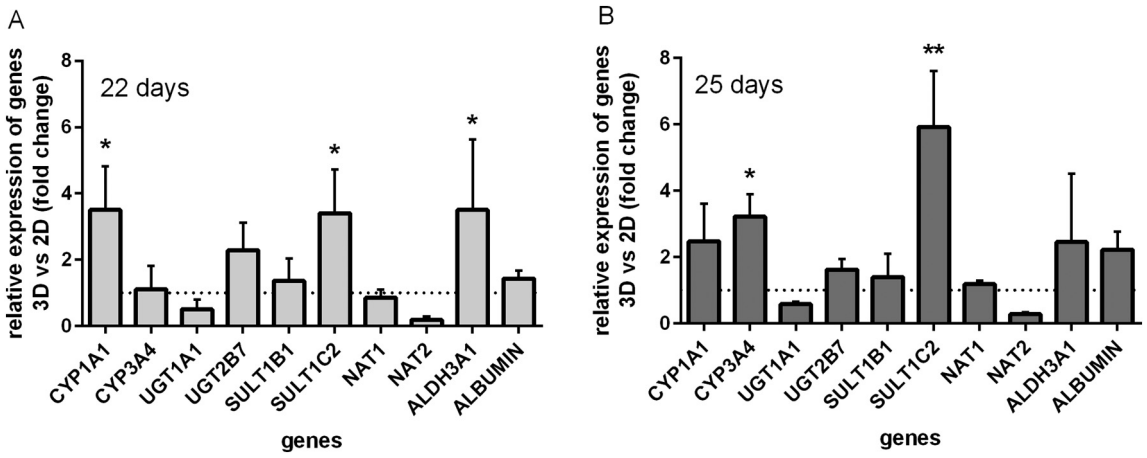


**Fig. 5.** Relative basal mRNA expression in 3D HepG2/C3A spheroids cultured under dynamic conditions for 22 (A) and 25 (B) days compared to 2-day old monolayer cultures. Data are presented as an average ± SD (N = 3). The dotted line denotes the expression of the corresponding gene in monolayer culture (1-fold change). A significant variance in mRNA expression in 3D compared to 2D cultures was assessed with the one-way ANOVA using multiple comparisons (Dunnett's) (* $p < 0.05$, ** $p < 0.01$).

to monolayer cultures. Therefore, our results are not surprising since the expression of genes in spheroids changes over time.

*3.3.2. The impact of model genotoxic compounds on mRNA level in HepG2/C3A spheroids*

Further, the changes in the transcription of studied genes involved in the metabolism (phase I and II), immediate early response and response to DNA damage were analysed after the exposure to genotoxic compounds. Relative mRNA level of the studied genes in treated groups compared to solvent controls are shown in Figs. 6 and 7.

Most of the xenobiotic-metabolizing enzymes are inducible (Braeuning et al., 2009; Denison and Whitlock, 1995; Mitchell and Warshawsky, 2003). Therefore, induction of the mRNA level of studied genes encoding phase I (*CYP3A4*, *CYP1A1*, *CYP1A2*, and *ALDH3A1*) and II (*UGT1A1*, *UGT2B7*, *SULT1C2*, *SULT1B1*, *NAT2*, *NAT1*) enzymes was investigated after the treatment of spheroids to B(*a*)P and PhIP for 24 or 96 h. B(*a*)P is primarily metabolized in the liver by human cytochromes (CYP1A1/CYP1B1) and epoxide hydrolase to carcinogenic intermediates that covalently bind to DNA to start the carcinogenic process (Melendez-Colon et al., 1999; Nebert et al., 2004; Qin and Meng, 2010; Whitlock, 1999). In HepG2/C3A spheroids, B(*a*)P after 24 h up-regulated the expression of *CYP3A4* (12.3-fold), *CYP1A1* (295.6-fold), *CYP1A2* (3.9-fold), *UGT1A1* (13.6-fold), *UGT2B7* (14.7-fold), *NAT2* (4.0-fold), *NAT1* (8.0-fold) and *ALDH3A1* (345.9-fold). This is in line

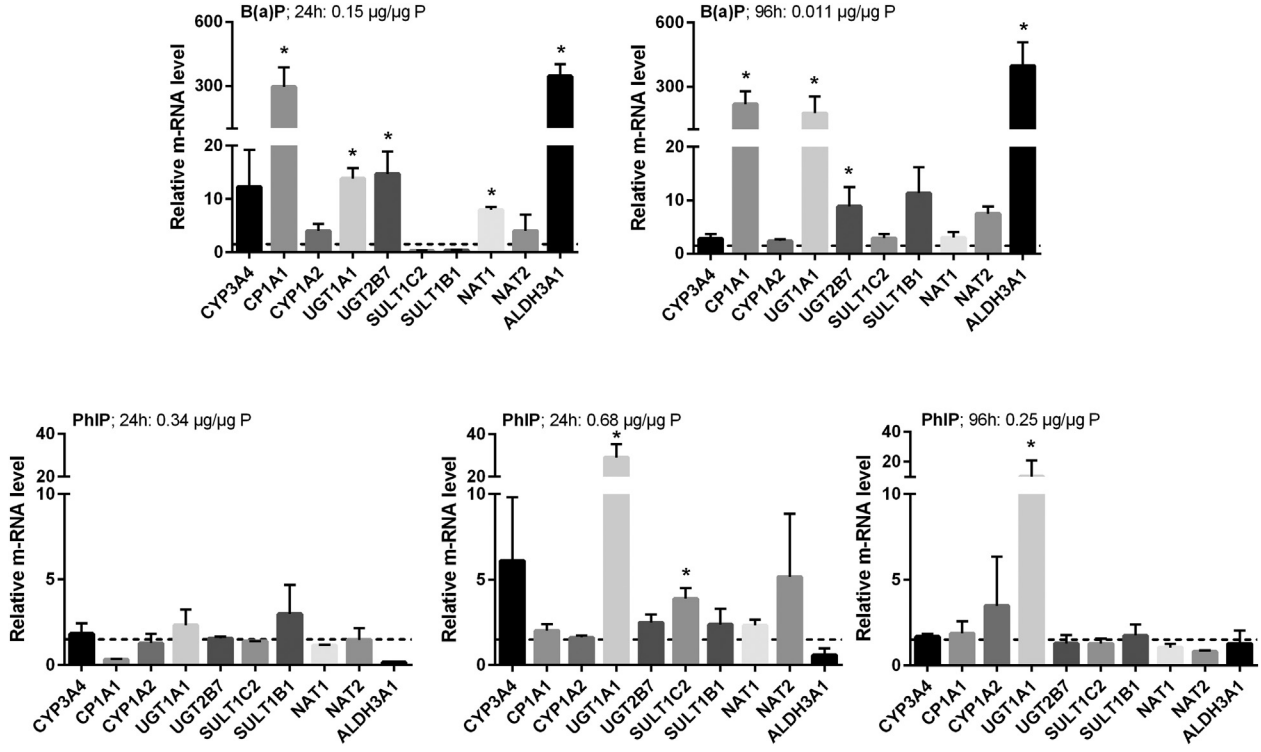


**Fig. 6.** The mRNA level of selected genes involved in the metabolism after 24 and 96 h of exposure of 21-day old HepG2/C3A spheroids to genotoxic compounds, B(*a*)P and PhIP. The dotted line denotes biologically significant differences in gene expression (1.5-fold change). The expression of each gene was assessed in duplicates and three independent experiments were performed. The statistical analysis between exposed and control groups was done by the multiple *t*-test analysis using the Sidak-Bonferroni method (* $p < 0.05$). An up-/down-regulation of ≥1.5 and ≤0.66-fold change, respectively, compared to the corresponding solvent control was considered a positive response.

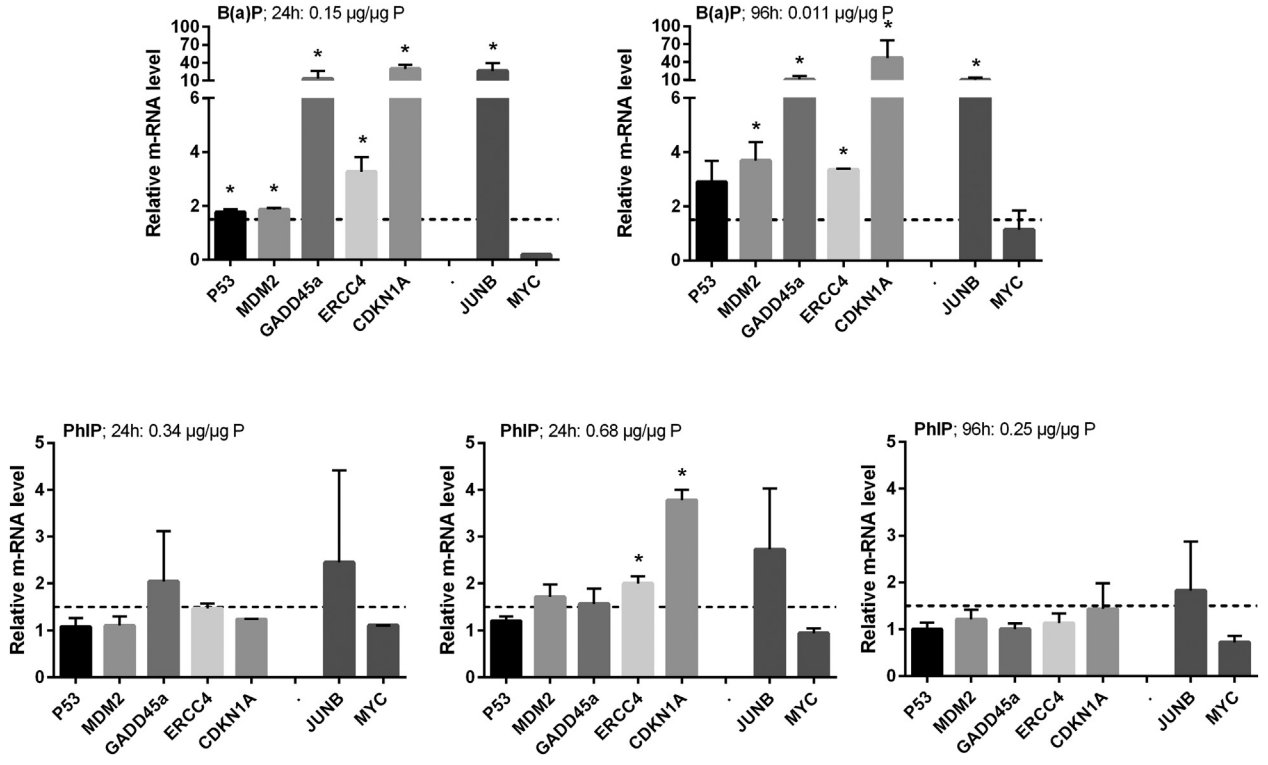


**Fig. 7.** The mRNA expression of studied genes involved in DNA damage response and the immediate-early response in 21-day old HepG2/C3A spheroids after 24 and 96 h of exposure to model genotoxic compounds. The dotted line denotes biologically significant differences in gene expression (1.5-fold change). The expression of each gene was assessed in duplicates and three experiments were done independently. The statistical variance was tested using the multiple *t*-tests and the Sidak-Bonferroni method (*$p < 0.05$). An up-/down-regulation of ≥1.5 and ≤0.66-fold change, respectively, compared to the control, was considered as a positive response.

with previous findings demonstrating that B(*a*)P in HepG2 monolayer cultures up-regulated genes encoding important cytochromes (*CYP1A1*, *CYP1A2*, and *CYP3A4*) (Bartosiewicz et al., 2001; Ewa and Danuta, 2017; Lee et al., 2006, 2009; Stiborová et al., 2014). Glucuronosyltransferases (UGTs), *N*-acetyltransferases (NATs) and sulfotransferases (SULT) belonging to phase II enzymes, act on the oxidized products generated from phase I and thus represent an important detoxification pathway (Gamage et al., 2006; Li et al., 2008). B(*a*)P up-regulated *UGT1A1* (13.8-fold), *UGT2B7* (14.6-fold), *NAT1* (7.9-fold) and *NAT2* (5.7-fold) and down-regulated *SULT1C2* (0.28-fold) and *SULT1B1* (0.36-fold). The up-regulation of *UGT1A1* by B(*a*)P has previously been observed in HepG2 cell monolayer cultures (Pezdirc et al., 2013) and in HepG2 spheroid cultures (Štampar et al., 2019). On the contrary, *NAT2* was not deregulated in HepG2 monolayer cultures (Pezdirc et al., 2013) and HepG2 spheroids (Štampar et al., 2019), while in the latter cell model *NAT1* was upregulated (Štampar et al., 2019).

PhIP is metabolized to a DNA-binding product by CYP1A2- and CYP1A1-catalyzed N-hydroxylation (Wilkening et al., 2003), while the major PhIP detoxification pathway is considered UGT-mediated glucuronidation and sulfotransferation and to a lesser extent *N*-acetyltransferation (Turesky, 2011; Turesky and Le Marchand, 2011). However, O-esterification of N-hydroxy-derivatives catalyzed by *N*-acetyltransferases (NATs) and sulfotransferases (SULTs) also produces N-acetoxy HAAs derivatives, which after heterocyclic cleavage produces DNA reactive nitrenium ion (Turesky, 2011). The 24-hour exposure of HepG2/C3A spheroids to PhIP was performed at two doses, 0.34 μg/μg P and 0.68 μg/μg P. At the lower dose PhIP up-regulated *CYP3A4* (1.8-fold), *UGT1A1* (2.3-fold) and *SULT1B1* (3.0-fold) and down-regulated *CYP1A1* (0.32-fold) and *ALDH3A1* (0.16-fold). In contrast, at 0.68 μg/μg P PhIP up-regulated phase I metabolic genes *CYP3A4* (6.1-fold), *CYP1A1* (6.0-fold) and *CYP1A2* (1.6-fold), and phase II metabolic genes *UGT1A1* (29.1-fold), *UGT2B7* (2.5-fold), *SULT1B1* (2.4-fold), *SULT1C2* (3.9-fold), *NAT1* (2.3-fold) and *NAT2* (5.2-fold), while *ALDH3A1* (0.74-fold) was not importantly deregulated. Similar metabolic gene deregulation by PhIP was described in metabolically competent HepaRG cells, where increased mRNA and activity levels of *CYP1A1*, *CYP1A2* and *CYP1B1* were described by Dumont et al. (2010). Presumably, this is the consequence of the activation of the aryl hydrocarbon receptor (AHR), the key nuclear factor in the regulation of CYPs and ALDHs (Omiecinski et al., 2011). Also in HepG2 monolayer cultures, PhIP up-regulated genes encoding phase I (*CYP1A1* and *CYP1A2)* (Pezdirc et al., 2013; Viegas et al., 2012) and phase II (*NAT2* and *UGT1A1)* (Pezdirc et al., 2013) metabolism, while *SULT1A1* was not expressed in HepG2 cells under the tested experimental conditions. The results of our study clearly demonstrate that in HepG2/C3A, spheroids *SULTs* were expressed at the mRNA level and were up-regulated upon PhIP exposure.

After 96 hour exposure, B(*a*)P up-regulated all studied genes involved in metabolism; *CYP3A4* (2.8-fold), *CYP1A1* (218.8-fold), *CYP1A2* (2.4-fold), *UGT1A1* (176.2-fold), *UGT2B7* (8.8-fold), *NAT1* (3.0-fold), *NAT2* (7.5-fold), *SULT1C2* (2.9-fold), *SULT1B1* (11.3-fold) and *ALDH3A1* (397.6-fold). The up-regulation of some of these genes was after 96 hour exposure more pronounced than after 24 h exposure to a higher dose. In PhIP (0.25 μg/μg P) exposed HepG2/C3A spheroids, *CYP1A2* (3.47-fold) and *UGT1A1* (10.35-fold) were up-regulated to a higher extend than after 24-hour exposure to 0.34 μg/μg P of PhIP (Fig. 6), while the expressions of other studied genes were not significantly different from their expressions in control spheroids. This may indicate that PhIP (0.25 μg/μg P) has been efficiently metabolized and detoxified during 96 h of exposure, which stopped upregulation of the expression of CYPs, SULTs, and NATs or the exposure dose was not high enough to up-regulate the expression of these enzymes.

The cellular response to the exposure to genotoxic chemicals depends on the cellular defence, particularly, DNA damage repair

mechanisms (Dumont et al., 2010). DNA damage triggers the activation of p53 network, where tumour suppressor p53 plays an essential role in controlling cellular proliferation in the context of DNA damage by activating the transcription of many crucial genes involved in cell cycle arrest and DNA repair, apoptosis, differentiation and senescence (Vogelstein et al., 2000). The cyclin-dependent kinase inhibitor 1A gene (*CDKN1A)* that encodes p21 is a p53-dependent key regulator of cell fate by triggering cell cycle arrest in G1 phase under multiple stress conditions including DNA damage (Warfel and El-Deiry, 2013). It is directly involved in DNA repair, including nucleotide excision repair (NER) (Cazzalini et al., 2010). The *GADD45α* is another gene that is regulated by p53 and is implicated in the regulation of several cellular functions, such as DNA damage and repair, cell cycle checkpoint, signalling transduction and maintenance of genomic stability (Tamura et al., 2012). It controls the cell cycle G2-M checkpoint, the DNA repair process and apoptosis (Wang et al., 1999). MDM2 protein, a product of a proto-oncogene, is under non-stressed conditions the negative regulation of *TP53* (Michael and Oren, 2002). It enhances the tumorigenicity of the cells and promotes survival of the cells and the progression of the cell cycle (Deb, 2003). The *ERCC4* gene has a vital role in DNA damage repair processes and in maintaining genomic stability. It is activated by DNA damaging compounds that induce covalent helix-distorting adducts and plays a central role in DNA NER (Manandhar et al., 2015). An important cellular response to carcinogens is also gene regulation *via* the transcription factor, the activator protein 1 (AP-1) that is composed of JUN and FOS protein dimers, known as homologs of retroviral oncoproteins. JUN-B is implicated in many essential cell processes, including differentiation, proliferation, and tumorigenesis (Hess et al., 2004). Another oncogene that is considered as a critical regulator of cell proliferation is *MYC*. Its deregulation is associated with the genesis of most human tumours (Adhikary and Eilers, 2005). The immediate-early response genes (*MYC* and *JUN*), which coordinate the expression of further genes required for subsequent cell cycle progression (Kohn, 1999), enable ligands of AHR to act as influential tumour promoters and carcinogens (Marlowe and Puga, 2005). Transcriptomic analyses revealed that in HepG2/C3A spheroids, exposure to B(*a*)P for 24 and 96 h caused transcriptional activation of *TP53* (1.8-fold and 2.9-fold, respectively), and its down-stream regulated genes *CDKN1A* (29.5-fold and 46.5-fold, respectively), *GADD45α* (13.5-fold and 10.4-fold, respectively) and *MDM2* (1.9-fold and 3.7-fold, respectively) as well as *ERCC4* (3.3-fold and 3.2-fold, respectively). Higher levels of the expressions of *TP53* and *CDKN1A* after prolonged exposure (96 h) correlate with the more pronounced increase of DNA damage after prolonged exposure. In HepG2 cells grown in monolayer, 24 hour exposure to B(*a*)P up-regulated the mRNA level of *CDKN1A* and *GADD45α*, whereas the expression of *TP53* was not affected, while *MDM2* was down-regulated (Pezdirc et al., 2013). In 21-day old spheroids at both 24 and 96 h of exposure, B(*a*)P up-regulated the expression of *JUNB* (26.4-fold and 9.5-fold, respectively), while *MYC* was significantly down-regulated (0.2-fold) after 24 h. Modifications in the expression of growth-related genes associated with the exposure to xenobiotics may be associated to tumorigenesis in target organs, for this reason, the significantly induced expression of *JUNB* by B(*a*)P may implicate the process of B(*a*)P induced carcinogenesis (Goldsworthy et al., 1994; Mehta, 1995). Altogether, the results showed that all genes associated with DNA damage response were greatly upregulated upon exposure to B(*a*)P at all applied conditions, which correlate with its genotoxic activity.

The heterocyclic aromatic amine PhIP after 24 hour exposure at dose 0.34 μg/μg P slightly, but not significantly upregulated only the expression of *GADD45α* (2.0-fold) and *JUNB* (2.45-fold). The higher dose of PhIP (0.68 μg/μg P) upregulated the expression of *CDKN1A1* (3.8-fold), *MDM2* (1.71-fold), *ERCC4* (2.0-fold) and *JUNB* (2.7-fold). The upregulation of *GADD45α* after exposure to PhIP was also described in HepG2 monolayer cultures (Pezdirc et al., 2013). After 96 h of exposure, no significant mRNA deregulation of genes involved in the response to DNA damage was observed, except for *JUNB* gene (1.8-fold), which belongs to immediate-early response genes (Fig. 7). These findings support the results obtained with the comet assay, where PhIP induced increased DNA strand break formation after 24 h but not after 96 hour exposure. These results imply the lower genotoxic potential of PhIP compared to BaP, as well as a different mechanism of action.

## 4. Conclusions

In recent years, considerable efforts have been brought to the development of a wide range of *in vitro* 3D cell models. These have shown promising results for their usage in drug discovery, stem cell research, cancer cell biology, and recently also in genetic and environmental toxicology to reduce disparities between the traditional 2D cell models and whole-animal systems. Moreover, *in vitro* 3D cell models can be used to fulfil the 3R (reduce, refine and replace) strategy to avoid unnecessary animal experiments with inaccurate predictions for humans due to species variability.

We optimized the comet assay method to determine the genotoxic activity of indirect-acting genotoxic compounds in 21-day old HepG2/C3A spheroids cultured in bioreactors under dynamic clinostat conditions and studied the effects of genotoxic compounds on the expression of genes encoding xenobiotic metabolic enzymes and enzymes involved in DNA damage and immediate-early response. The dynamic clinostat culturing conditions that allow growth and generation of a high amount of uniform spheroids for a prolonged time without the addition of extracellular matrix enable a constant supply of nutrients entering the spheroid. The formed spheroids enable long-term exposure studies where low for human exposure relevant doses of chemicals including complex environmental mixtures can be applied. Based on the results of our study, 21-day old HepG2/C3A spheroids proved to be metabolically competent; the basal levels of mRNA of the studied genes encoding phase I and phase II metabolic enzymes were significantly higher in 3D cultures compared to 2D cultures. The 3D spheroids also responded to the exposure to indirect-acting model environmental pollutants, benzo(*a*)pyrene [B(*a*)P], and 2-amino-1-methyl-6-phenylimidazo(4,5-*b*)pyridine [PhIP] with compound-specific mRNA deregulation of those genes. The genotoxic activity of B(*a*)P and PhIP was confirmed in HepG2/C3A spheroids after short and prolonged exposure. Both compounds induced increased DNA strand break formation and compound-specific deregulation of the expression of DNA damage and immediate-early responsive genes. Our study demonstrated that high viability of HepG2/C3A spheroids and the dynamic 3D model enables their use for prolonged exposure studies, which is of great importance for detecting and predicting the genotoxic effects relevant for chronic human exposure to a low dose of genotoxic compounds, which can be found in the human environment. Therefore, the HepG2/C3A 3D cell model cultured under dynamic conditions, as a result of more complex structure and better metabolic capacity, represents a very sensitive system and can provide more physiologically important information and more predictive information for human health risk assessment and therefore, can contribute to more trustworthy genotoxicity assessment of chemicals and complex environmental samples.

## Funding

This research was funded by grants P1-0245, J1-2465 and grant to young researchers MR-MStampar of the Slovenian Research Agency ARRS, and COST Action CA16119 (*In vitro* 3-D total cell guidance and fitness). HSF was supported by a PhD grant from Sino Danish Centre for Education and Research.

## CRediT authorship contribution statement

**Martina Štampar:** Conceptualization, Methodology, Software, Validation, Formal analysis, Investigation, Data curation, Writing - original draft, Visualization. **Helle Sedighi Frandsen:** Methodology, Software, Validation, Investigation, Data curation, Writing - review & editing, Visualization. **Adelina Rogowska-Wrzesinska:** Conceptualization, Methodology, Formal analysis, Investigation, Resources, Writing - review & editing, Funding acquisition. **Krzysztof Wrzesinski:** Methodology, Writing - review & editing. **Metka Filipič:** Resources, Writing - review & editing, Supervision, Project administration, Funding acquisition. **Bojana Žegura:** Conceptualization, Methodology, Validation, Formal analysis, Investigation, Resources, Data curation, Writing - original draft, Visualization, Supervision, Project administration, Funding acquisition.

## Declaration of competing interest

The authors declare that they have no known competing financial interests or personal relationships that could have appeared to influence the work reported in this paper.

## References


Adhikary, S., Eilers, M., 2005. Transcriptional regulation and transformation by Myc proteins. Nat. Rev. Mol. Cell Biol. https://doi.org/10.1038/nrm1703.

Aucamp, J., Calitz, C., Bronkhorst, A.J., Wrzesinski, K., Hamman, S., Gouws, C., Pretorius, P.J., 2017. Cell-free DNA in a three-dimensional spheroid cell culture model: a preliminary study. Int. J. Biochem. Cell Biol. 89, 182–192. https://doi.org/10.1016/j.biocel.2017.06.014.

Baan, R., Grosse, Y., Straif, K., Secretan, B., El Ghissassi, F., Bouvard, V., Benbrahim-Tallaa, L., Guha, N., Freeman, C., Galichet, L., Cogliano, V., 2009. A review of human carcinogens–part F: chemical agents and related occupations. Lancet Oncol. https://doi.org/10.1016/s1470-2045(09)70358-4.

Baebler, Š., Svalina, M., Petek, M., Stare, K., Rotter, A., Pompe-Novak, M., Gruden, K., 2017. quantGenius: implementation of a decision support system for qPCR-based gene quantification. BMC Bioinformatics 18, 276. https://doi.org/10.1186/s12859-017-1688-7.

Baird, W.M., Hooven, L.A., Mahadevan, B., 2005. Carcinogenic polycyclic aromatic hydrocarbon-DNA adducts and mechanism of action. Environ. Mol. Mutagen. https://doi.org/10.1002/em.20095.

Bartosiewicz, M., Penn, S., Buckpitt, A., 2001. Applications of gene arrays in environmental toxicology: fingerprints of gene regulation associated with cadmium chloride, benzo (a)pyrene, and trichloroethylene. Environ. Health Perspect. 109, 71–74. https://doi.org/10.1289/ehp.0110971.

Basu, A., Dydowiczová, A., Čtveráčková, L., Jaša, L., Trosko, J.E., Bláha, L., Babica, P., 2018. Assessment of hepatotoxic potential of cyanobacterial toxins using 3D in vitro model of adult human liver stem cells. Environ. Sci. Technol. 52, 10078–10088. https://doi.org/10.1021/acs.est.8b02291.

Basu, A., Dydowiczová, A., Trosko, J.E., Bláha, L., Babica, P., 2020. Ready to go 3D? A semi-automated protocol for microwell spheroid arrays to increase scalability and throughput of 3D cell culture testing. Toxicol. Mech. Methods (0), 1–43 https://doi.org/10.1080/15376516.2020.1800881.

Braeuning, A., Sanna, R., Huelsken, J., Schwarz, M., 2009. Inducibility of drug-metabolizing enzymes by xenobiotics in mice with liver-specific knockout of ctnnb1. Drug Metab. Dispos. 37, 1138–1145. https://doi.org/10.1124/dmd.108.026179.

Breslin, S., O'Driscoll, L., 2013. Three-dimensional cell culture: the missing link in drug discovery. Drug Discov. Today 18, 240–249. https://doi.org/10.1016/j.drudis.2012.10.003.

Burden, N., Chapman, K., Sewell, F., Robinson, V., 2015. Pioneering better science through the 3Rs: an introduction to the National Centre for the Replacement, Refinement, and Reduction of Animals in Research (NC3Rs). J. Am. Assoc. Lab. Anim. Sci. 54, 198–208.

Cazzalini, O., Scovassi, A.I., Savio, M., Stivala, L.A., Prosperi, E., 2010. Multiple roles of the cell cycle inhibitor p21(CDKN1A) in the DNA damage response. Mutat. Res. 704, 12–20. https://doi.org/10.1016/j.mrrev.2010.01.009.

Chang, T.T., Hughes-Fulford, M., 2009. Monolayer and spheroid culture of human liver hepatocellular carcinoma cell line cells demonstrate distinct global gene expression patterns and functional phenotypes. Tissue Eng. Part A 15, 559–567. https://doi.org/10.1089/ten.tea.2007.0434.

Corvi, R., Madia, F., 2017. In vitro genotoxicity testing–can the performance be enhanced? Food Chem. Toxicol. 106, 600–608. https://doi.org/10.1016/j.fct.2016.08.024.

Deb, S.P., 2003. Cell cycle regulatory functions of the human oncoprotein MDM2. Mol. Cancer Res. 1, 1009–1016.

Denison, M.S., Whitlock, J.P., 1995. Xenobiotic-inducible transcription of cytochrome P450 genes. J. Biol. Chem. https://doi.org/10.1074/jbc.270.31.18175.

Dix, D.J., Houck, K.A., Martin, M.T., Richard, A.M., Setzer, R.W., Kavlock, R.J., 2007. The toxcast program for prioritizing toxicity testing of environmental chemicals. Toxicol. Sci. 95, 5–12. https://doi.org/10.1093/toxsci/kfl103.

Dumont, J., Jossé, R., Lambert, C., Anthérieu, S., Laurent, V., Loyer, P., Robin, M.A., Guillouzo, A., 2010. Preferential induction of the AhR gene battery in HepaRG cells after a single or repeated exposure to heterocyclic aromatic amines. Toxicol. Appl. Pharmacol. 249, 91–100. https://doi.org/10.1016/j.taap.2010.08.027.

Edmondson, R., Broglie, J.J., Adcock, A.F., Yang, L., 2014. Three-dimensional cell culture systems and their applications in drug discovery and cell-based biosensors. Assay Drug Dev. Technol. 12, 207–218. https://doi.org/10.1089/adt.2014.573.

Elje, E., Hesler, M., Rundén-Pran, E., Mann, P., Mariussen, E., Wagner, S., Dusinska, M., Kohl, Y., 2019. The comet assay applied to HepG2 liver spheroids. Mutat. Res. - Genet. Toxicol. Environ. Mutagen. 845, 403033. https://doi.org/10.1016/j.mrgentox.2019.03.006.

Ewa, B., Danuta, M.Š., 2017. Polycyclic aromatic hydrocarbons and PAH-related DNA adducts. J. Appl. Genet. https://doi.org/10.1007/s13353-016-0380-3.

Fey, S.J., Wrzesinski, K., 2012. Determination of drug toxicity using 3D spheroids constructed from an immortal human hepatocyte cell line. Toxicol. Sci. 127, 403–411. https://doi.org/10.1093/toxsci/kfs122.

Flampouri, E., Imar, S., Oconnell, K., Singh, B., 2019. Spheroid-3D and monolayer-2D intestinal electrochemical biosensor for toxicity/viability testing: applications in drug screening, food safety, and environmental pollutant analysis. ACS Sensors 4, 660–669. https://doi.org/10.1021/acssensors.8b01490.

Gajski, G., Gerić, M., Žegura, B., Novak, M., Nunić, J., Bajrektarević, D., Garaj-Vrhovac, V., Filipič, M., 2016. Genotoxic potential of selected cytostatic drugs in human and zebrafish cells. Environ. Sci. Pollut. Res. 23, 14739–14750. https://doi.org/10.1007/s11356-015-4592-6.

Gamage, N., Barnett, A., Hempel, N., Duggleby, R.G., Windmill, K.F., Martin, J.L., McManus, M.E., 2006. Human sulfotransferases and their role in chemical metabolism. Toxicol. Sci. https://doi.org/10.1093/toxsci/kfj061.

Goldsworthy, T.L., Goldsworthy, S.M., Sprankle, C.S., Butterworth, B.E., 1994. Expression of myc, fos and Ha-ras associated with chemically induced cell proliferation in the rat liver. Cell Prolif. 27, 269–278. https://doi.org/10.1111/j.1365-2184.1994.tb01424.x.

Gong, X., Lin, C., Cheng, J., Su, J., Zhao, H., Liu, T., Wen, X., Zhao, P., 2015. Generation of multicellular tumor spheroids with microwell-based agarose scaffolds for drug testing. PLoS One 10, e0130348. https://doi.org/10.1371/journal.pone.0130348.

Hartig, T., Mitchell, R., De Vries, S., Frumkin, H., 2014. Nature and health. Annual Review of Public Health. Annual Reviews Inc., pp. 207–228 https://doi.org/10.1146/annurev-publhealth-032013-182443.

Hercog, K., Štampar, M., Štern, A., Filipič, M., Žegura, B., 2020. Application of advanced HepG2 3D cell model for studying genotoxic activity of cyanobacterial toxin cylindrospermopsin. Environ. Pollut. 265, 114965. https://doi.org/10.1016/j.envpol.2020.114965.

Hess, J., Angel, P., Schorpp-Kistner, M., 2004. AP-1 subunits: quarrel and harmony among siblings. J. Cell Sci. 117, 5965–5973. https://doi.org/10.1242/jcs.01589.

Hurrell, T., Lilley, K.S., Cromarty, A.D., 2019. Proteomic responses of HepG2 cell monolayers and 3D spheroids to selected hepatotoxins. Toxicol. Lett. 300, 40–50. https://doi.org/10.1016/j.toxlet.2018.10.030.

Iyer, V.V., Yang, H., Ierapetritou, M.G., Roth, C.M., 2010. Effects of glucose and insulin on HepG2-C3A cell metabolism. Biotechnol. Bioeng. 107, 347–356. https://doi.org/10.1002/bit.22799.

Kirkland, D., Pfuhler, S., Tweats, D., Aardema, M., Corvi, R., Darroudi, F., Elhajouji, A., Glatt, H., Hastwell, P., Hayashi, M., Kasper, P., Kirchner, S., Lynch, A., Marzin, D., Maurici, D., Meunier, J.-R., Müller, L., Nohynek, G., Parry, J., Parry, E., Thybaud, V., Tice, R., van Benthem, J., Vanparys, P., White, P., 2007. How to reduce false positive results when undertaking in vitro genotoxicity testing and thus avoid unnecessary follow-up animal tests: report of an ECVAM Workshop. Mutat. Res. Toxicol. Environ. Mutagen. 628, 31–55. https://doi.org/10.1016/J.MRGENTOX.2006.11.008.

Kohn, K.W., 1999. Molecular interaction map of the mammalian cell cycle control and DNA repair systems. Mol. Biol. Cell 10, 2703–2734. https://doi.org/10.1091/mbc.10.8.2703.

Lee, C.M., Chen, S.Y., Lee, Y.C.G., Huang, C.Y.F., Chen, Y.M.A., 2006. Benzo[a]pyrene and glycine N-methyltransferse interactions: gene expression profiles of the liver detoxification pathway. Toxicol. Appl. Pharmacol. 214, 126–135. https://doi.org/10.1016/j.taap.2005.12.020.

Lee, J., Lilly, G.D., Doty, R.C., Podsiadlo, P., Kotov, N.A., 2009. In vitro toxicity testing of nanoparticles in 3D cell culture. Small 5, 1212–1221. https://doi.org/10.1002/smll.200801788.

Li, Y., Lindsay, J., Wang, L.-L., Zhou, S.-F., 2008. Structure, function and polymorphism of human cytosolic sulfotransferases. Curr. Drug Metab. 9, 99–105. https://doi.org/10.2174/138920008783571819.

Lin, Ruei-Zeng, Lin, Ruei-Zhen, Chang, H.-Y., 2008. Recent advances in three-dimensional multicellular spheroid culture for biomedical research. Biotechnol. J. 3, 1172–1184. https://doi.org/10.1002/biot.200700228.

Loessner, D., Stok, K.S., Lutolf, M.P., Hutmacher, D.W., Clements, J.A., Rizzi, S.C., 2010. Bioengineered 3D platform to explore cell-ECM interactions and drug resistance of epithelial ovarian cancer cells. Biomaterials 31, 8494–8506. https://doi.org/10.1016/j.biomaterials.2010.07.064.

Manabe, S., Kurihara, N., Wada, O., Izumikawa, S., Asakuno, K., Morita, M., 1993. Detection of a carcinogen, 2-amino-1-methyl-6-phenylimidazo [4,5-b]pyridine, in airborne particles and diesel-exhaust particles. Environ. Pollut. 80, 281–286. https://doi.org/10.1016/0269-7491(93)90049-T.

Manandhar, M., Boulware, K.S., Wood, R.D., 2015. The ERCC1 and ERCC4 (XPF) genes and gene products. Gene. https://doi.org/10.1016/j.gene.2015.06.026.

Mandon, M., Huet, S., Dubreil, E., Fessard, V., Le Hégarat, L., 2019. Three-dimensional HepaRG spheroids as a liver model to study human genotoxicity in vitro with the single cell gel electrophoresis assay. Sci. Rep. 9. https://doi.org/10.1038/s41598-019-47114-7.

Marlowe, J.L., Puga, A., 2005. Aryl hydrocarbon receptor, cell cycle regulation, toxicity, and tumorigenesis. J. Cell. Biochem. 96, 1174–1184. https://doi.org/10.1002/jcb.20656.
Mehta, R., 1995. The potential for the use of cell proliferation and oncogene expression as intermediate markers during liver carcinogenesis. Cancer Lett. 93, 85–102. https://doi.org/10.1016/0304-3835(95)03790-4.
Melendez-Colon, V.J., Luch, A., Seidel, A., Baird, W.M., 1999. Cancer initiation by polycyclic aromatic hydrocarbons results from formation of stable DNA adducts rather than apurinic sites. Carcinogenesis 20, 1885–1891. https://doi.org/10.1093/carcin/20.10.1885.
Michael, D., Oren, M., 2002. The p53 and Mdm2 families in cancer. Curr. Opin. Genet. Dev. 12, 53–59. https://doi.org/10.1016/s0959-437x(01)00264-7.
Mitchell, K.R., Warshawsky, D., 2003. Xenobiotic inducible regions of the human arylamine N-acetyltransferase 1 and 2 genes. Toxicol. Lett. 139, 11–23. https://doi.org/10.1016/S0378-4274(02)00437-X.
Naccari, C., Galceran, M.T., Moyano, E., Cristani, M., Siracusa, L., Trombetta, D., 2009. Presence of heterocyclic aromatic amines (HAS) in smoked "Provola" cheese from Calabria (Italy). Food Chem. Toxicol. 47, 321–327. https://doi.org/10.1016/j.fct.2008.11.018.
Nebert, D.W., Dalton, T.P., Okey, A.B., Gonzalez, F.J., 2004. Role of aryl hydrocarbon receptor-mediated induction of the CYP1 enzymes in environmental toxicity and cancer. J. Biol. Chem. https://doi.org/10.1074/jbc.R400004200.
Nibourg, G.A.A., Chamuleau, R.A.F.M., Van Gulik, T.M., Hoekstra, R., 2012. Proliferative human cell sources applied as biocomponent in bioartificial livers: a review. Expert. Opin. Biol. Ther. https://doi.org/10.1517/14712598.2012.685714.
Omiecinski, C.J., Vanden Heuvel, J.P., Perdew, G.H., Peters, J.M., 2011. Xenobiotic metabolism, disposition, and regulation by receptors: from biochemical phenomenon to predictors of major toxicities. Toxicol. Sci. 120 (Suppl. 1), S49–S75. https://doi.org/10.1093/toxsci/kfq338.
Pezdirc, M., Žegura, B., Filipič, M., 2013. Genotoxicity and induction of DNA damage responsive genes by food-borne heterocyclic aromatic amines in human hepatoma HepG2 cells. Food Chem. Toxicol. 59, 386–394. https://doi.org/10.1016/j.fct.2013.06.030.
Pfuhler, S., Kirkland, D., Kasper, P., Hayashi, M., Vanparys, P., Carmichael, P., Dertinger, S., Eastmond, D., Elhajouji, A., Krul, C., Rothfuss, A., Schoening, G., Smith, A., Speit, G., Thomas, C., van Benthem, J., Corvi, R., 2009. Reduction of use of animals in regulatory genotoxicity testing: identification and implementation opportunities-report from an ECVAM workshop. Mutat. Res. - Genet. Toxicol. Environ. Mutagen. 680, 31–42. https://doi.org/10.1016/j.mrgentox.2009.09.002.
Pfuhler, S., van Benthem, J., Curren, R., Doak, S.H., Dusinska, M., Hayashi, M., Heflich, R.H., Kidd, D., Kirkland, D., Luan, Y., Ouedraogo, G., Reisinger, K., Sofuni, T., van Acker, F., Yang, Y., Corvi, R., 2020. Use of in vitro 3D tissue models in genotoxicity testing: Strategic fit, validation status and way forward. Report of the Working Group From the 7th International Workshop on Genotoxicity Testing (IWGT). Mutagen, Mutat. Res. - Genet. Toxicol. Environ https://doi.org/10.1016/j.mrgentox.2020.503135.
Piccinini, F., Tesei, A., Arienti, C., Bevilacqua, A., 2015. Cancer multicellular spheroids: volume assessment from a single 2D projection. Comput. Methods Prog. Biomed. 118, 95–106. https://doi.org/10.1016/j.cmpb.2014.12.003.
Qin, G., Meng, Z., 2010. Sulfur dioxide and benzo(a)pyrene modulates CYP1A and tumor-related gene expression in rat liver. Environ. Toxicol. 25, 169–179. https://doi.org/10.1002/tox.20484.
Ramaiahgari, S.C., Den Braver, M.W., Herpers, B., Terpstra, V., Commandeur, J.N.M., Van De Water, B., Price, L.S., 2014. A 3D in vitro model of differentiated HepG2 cell spheroids with improved liver-like properties for repeated dose high-throughput toxicity studies. Arch. Toxicol. 88, 1083–1095. https://doi.org/10.1007/s00204-014-1215-9.
Ramaiahgari, S.C., Waidyanatha, S., Dixon, D., DeVito, M.J., Paules, R.S., Ferguson, S.S., 2017. Three-dimensional (3D) HepaRG spheroid model with physiologically relevant xenobiotic metabolism competence and hepatocyte functionality for liver toxicity screening. Toxicol. Sci. 159, 124–136. https://doi.org/10.1093/toxsci/kfx122.
Schechtman, L.M., 2002. Implementation of the 3Rs (refinement, reduction, and replacement): validation and regulatory acceptance considerations for alternative toxicological test methods. ILAR J. 43, S85–S94. https://doi.org/10.1093/ilar.43.suppl_1.s85.
Shah, U.-K., Mallia, J. de O., Singh, N., Chapman, K.E., Doak, S.H., Jenkins, G.J.S., 2018. A three-dimensional in vitro HepG2 cells liver spheroid model for genotoxicity studies. Mutat. Res. Toxicol. Environ. Mutagen. 825, 51–58. https://doi.org/10.1016/J.MRGENTOX.2017.12.005.
Skog, K., Solyakov, A., Arvidsson, P., Jägerstad, M., 1998. Analysis of nonpolar heterocyclic amines in cooked foods and meat extracts using gas chromatography-mass spectrometry. J. Chromatogr. A 803, 227–233. https://doi.org/10.1016/S0021-9673(97)01266-1.
Snykers, S., De Kock, J., Rogiers, V., Vanhaecke, T., 2009. In vitro differentiation of embryonic and adult stem cells into hepatocytes: state of the art. Stem Cells 27, 577–605. https://doi.org/10.1634/stemcells.2008-0963.
Štampar, M., Tomc, J., Filipič, M., Žegura, B., 2019. Development of in vitro 3D cell model from hepatocellular carcinoma (HepG2) cell line and its application for genotoxicity testing. Arch. Toxicol. 93, 3321–3333. https://doi.org/10.1007/s00204-019-02576-6.
Stiborová, M., Moserová, M., Černá, V., Indra, R., Dračínský, M., Šulc, M., Henderson, C.J., Wolf, C.R., Schmeiser, H.H., Phillips, D.H., Frei, E., Arlt, V.M., 2014. Cytochrome b5 and epoxide hydrolase contribute to benzo[a]pyrene-DNA adduct formation catalyzed by cytochrome P450 1A1 under low NADPH:P450 oxidoreductase conditions. Toxicology 318, 1–12. https://doi.org/10.1016/j.tox.2014.02.002.
Štraser, A., Filipič, M., Žegura, B., 2011. Genotoxic effects of the cyanobacterial hepatotoxin cylindrospermopsin in the HepG2 cell line. Arch. Toxicol. 85, 1617–1626. https://doi.org/10.1007/s00204-011-0716-z.
Sun, H., Wei, Y., Deng, H., Xiong, Q., Li, M., Lahiri, J., Fang, Y., 2014. Label-free cell phenotypic profiling decodes the composition and signaling of an endogenous ATP-sensitive potassium channel. Sci. Rep. 4. https://doi.org/10.1038/srep04934.
Tamta, H., Pawar, R.S., Wamer, W.G., Grundel, E., Krynitsky, A.J., Rader, J.I., 2012. Comparison of metabolism-mediated effects of pyrrolizidine alkaloids in a HepG2/C3A cell-S9 co-incubation system and quantification of their glutathione conjugates. Xenobiotica 42, 1038–1048. https://doi.org/10.3109/00498254.2012.679978.
Tamura, R.E., de Vasconcellos, J.F., Sarkar, D., Libermann, T.A., Fisher, P.B., Zerbini, L.F., 2012. GADD45 proteins: central players in tumorigenesis. Curr. Mol. Med. 12, 634–651. https://doi.org/10.2174/156652412800619978.
Turesky, R.J., 2011. Heterocyclic aromatic amines: potential human carcinogens. Curr. Cancer Res. 6, 95–112. https://doi.org/10.1007/978-1-61737-995-6_5.
Turesky, R.J., Le Marchand, L., 2011. Metabolism and biomarkers of heterocyclic aromatic amines in molecular epidemiology studies: lessons learned from aromatic amines. Chem. Res. Toxicol. 24, 1169–1214. https://doi.org/10.1021/tx200135s.
Tvardovskiy, A., Wrzesinski, K., Sidoli, S., Fey, S.J., Rogowska-Wrzesinska, A., Jensen, O.N., 2015. Top-down and middle-down protein analysis reveals that intact and clipped human histones differ in post-translational modification patterns. Mol. Cell. Proteomics 14, 3142–3153. https://doi.org/10.1074/mcp.M115.048975.
Viegas, O., Žegura, B., Pezdric, M., Novak, M., Ferreira, I.M.P.L.V.O., Pinho, O., Filipič, M., 2012. Protective effects of xanthohumol against the genotoxicity of heterocyclic aromatic amines MeIQx and PhIP in bacteria and in human hepatoma (HepG2) cells. Food Chem. Toxicol. 50, 949–955. https://doi.org/10.1016/j.fct.2011.11.031.
Vogelstein, B., Lane, D., Levine, A.J., 2000. Surfing the p53 network. Nature 408, 307–310. https://doi.org/10.1038/35042675.
Wang, X.W., Zhan, Q., Coursen, J.D., Khan, M.A., Kontny, H.U., Yu, L., Hollander, M.C., O'Connor, P.M., Fornace, A.J., Harris, C.C., 1999. GADD45 induction of a G2/M cell cycle checkpoint. Proc. Natl. Acad. Sci. U. S. A. 96, 3706–3711. https://doi.org/10.1073/pnas.96.7.3706.
Warfel, N.A., El-Deiry, W.S., 2013. P21WAF1 and tumourigenesis: 20 years after. Curr. Opin. Oncol. https://doi.org/10.1097/CCO.0b013e32835b639e.
Whitlock, J.P., 1999. Induction of cytochrome P4501A1. Annu. Rev. Pharmacol. Toxicol. 39, 103–125. https://doi.org/10.1146/annurev.pharmtox.39.1.103.
Wilkening, S., Stahl, F., Augustinous, B., 2003. Hepg2 with regard to their biotransformation properties. Drug Metab. Dispos. 31, 1035–1042.
Wojdyla, K., Wrzesinski, K., Williamson, J., Fey, S.J., Rogowska-Wrzesinska, A., 2016. Acetaminophen-induced: S -nitrosylation and S -sulfenylation signalling in 3D cultured hepatocarcinoma cell spheroids. Toxicol. Res. (Camb). 5, 905–920. https://doi.org/10.1039/c5tx00469a.
Wong, S.F., No, D.Y., Choi, Y.Y., Kim, D.S., Chung, B.G., Lee, S.H., 2011. Concave microwell based size-controllable hepatosphere as a three-dimensional liver tissue model. Biomaterials 32, 8087–8096. https://doi.org/10.1016/j.biomaterials.2011.07.028.
Wrzesinski, K., Fey, S.J., 2013. After trypsinisation, 3D spheroids of C3A hepatocytes need 18 days to re-establish similar levels of key physiological functions to those seen in the liver. Toxicol. Res. (Camb). 2, 123–135. https://doi.org/10.1039/c2tx20060k.
Wrzesinski, K., Fey, S.J., 2015. From 2D to 3D - a new dimension for modelling the effect of natural products on human tissue. Curr. Pharm. Des. 21, 5605–5616. https://doi.org/10.2174/1381612821666151002114227.
Wrzesinski, K., Magnone, M.C., Hansen, L.V., Kruse, M.E., Bergauer, T., Bobadilla, M., Gubler, M., Mizrahi, J., Zhang, K., Andreasen, C.M., Joensen, K.E., Andersen, S.M., Olesen, J.B., Schaffalitzky de Muckadell, O.B., Fey, S.J., 2013. HepG2/C3A 3D spheroids exhibit stable physiological functionality for at least 24 days after recovering from trypsinisation. Toxicol. Res. (Camb). 2, 163. https://doi.org/10.1039/c3tx20086h.
Wrzesinski, K., Rogowska-Wrzesinska, A., Kanlaya, R., Borkowski, K., Schwämmle, V., Dai, J., Joensen, K.E., Wojdyla, K., Carvalho, V.B., Fey, S.J., 2014. The cultural divide: exponential growth in classical 2D and metabolic equilibrium in 3D environments. PLoS One 9. https://doi.org/10.1371/journal.pone.0106973.
Yang, Y., Tang, X., Hao, F., Ma, Z., Wang, Y., Wang, L., Gao, Y., 2018. Bavachin induces apoptosis through mitochondrial regulated ER stress pathway in HepG2 cells. Biol. Pharm. Bull. 41, 198–207. https://doi.org/10.1248/bpb.b17-00672.
Young, C.K.J., Young, M.J., 2019. Comparison of HepaRG cells following growth in proliferative and differentiated culture conditions reveals distinct bioenergetic profiles. Cell Cycle 18, 476–499. https://doi.org/10.1080/15384101.2019.1578133.
Žegura, B., Heath, E., Černoša, A., Filipič, M., 2009. Combination of in vitro bioassays for the determination of cytotoxic and genotoxic potential of wastewater, surface water and drinking water samples. Chemosphere 75, 1453–1460. https://doi.org/10.1016/j.chemosphere.2009.02.041.